Study of the process $e^+e^- \to \pi^+\pi^-\pi^0\pi^0$ at energies $\sqrt{s} < 1$ GeV*

M. N. Achasov[1,2]　K. I. Beloborodov[1,2]　A. V. Berdyugin[1]　A. A. Botov[1]　V. B. Golubev[1,2]

T. V. Dimova[1,2]　V. P. Druzhinin[1,2]　L. V. Kardapoltsev[1,2]　A. G. Kharlamov [1,2;1)]　D. P. Kovrizhin[1]

I. A. Koop[1,2]　A. A. Korol[1,2]　S. V. Koshuba[1]　A. E. Obrazovsky[1,2]　E. V. Pakhtusova[1]　D. A. Shtol[1]

S. I. Serednyakov[1,2]　Z. K. Silagadze[1,2]　A. N. Skrinsky[1]　Yu. A. Tikhonov[1,2]　Yu. M. Shatunov[1]

A. V. Vasil'ev[1,2]

[1] Budker Institute of Nuclear Physics, Russian Academy of Sciences, Siberian Branch,
pr. Akademika Lavrent'eva 11, Novosibirsk, 630090 Russia
[2] Novosibirsk State University, Novosibirsk, 630090 Russia

Abstract　In an experiment with the Spherical Neutral Detector at VEPP-2M collider the cross section of the process $e^+e^- \to \pi^+\pi^-\pi^0\pi^0$ was measured. At energies $\sqrt{s} < 920$ MeV this cross section was measured for the first time. The energy dependence of the cross section is well discribed by the vector dominance model with contributions from ρ, ρ', ρ'' mesons. The decay probability $\rho \to \pi^+\pi^-\pi^0\pi^0$ was found to be $B_\rho = (1.60 \pm 0.74 \pm 0.18) \times 10^{-5}$. The upper limit for the decay $\omega \to \pi^+\pi^-\pi^0\pi^0$ was improved by two orders of magnitude compared to the previous measurements and is $B_\omega < 2 \times 10^{-4}$ at 90% confidence level.

Key words　VEPP-2M, spherical neutral detector, meson decay

PACS　13.66.Bc, 13.60.Hb, 13.25.Jx, 12.40.Vv

1　Introduction

The cross section of the process $e^+e^- \to \pi^+\pi^-\pi^0\pi^0$ at energies $\sqrt{s} < 1$ GeV is determined by the transition of vector mesons $V(\rho,\ \rho',\ \rho'')$ to the four π-mesons. The main intermediate states are $\omega\pi^0$ and $a_1\pi$; the intermediate mechanism $\sigma\rho$ could also present at these energies; the diagrams for these processes are shown in Fig. 1

At energies below 1 GeV, the experimental data on the process $e^+e^- \to \pi^+\pi^-\pi^0\pi^0$ are poor [1]. Charged channel $e^+e^- \to \pi^+\pi^-\pi^+\pi^-$ was studied slightly better in this energy range [2]. Simultaneous analysis of these cross sections would allow to extract coupling constants of ρ-meson with four π-mesons.

The decay $\omega \to \pi^+\pi^-\pi^0\pi^0$ forbidden by isospin conservation is very intresting. The present upper limit for the relative probability of this decay is ruther soft [3] to search for. Unfortunately, there are no theoretical predictions for the probability of this decay.
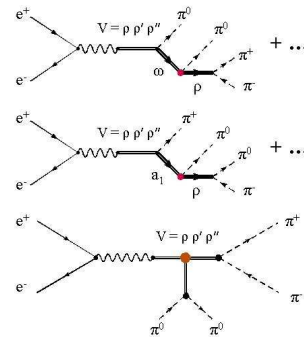

Fig. 1.　Diagrams for the transition $e^+e^- \to \pi^+\pi^-\pi^0\pi^0$.

2　Experiment

The Spherical Neutral Detector (SND) [4] was taking data from 1995 to 2000 at the VEPP2M collider [5] in the energy range 360–1400 MeV. The detector includes several subsystems. The tracking system consists of two cylindrical jet-type drift chambers. The angular resolution is $1.8°$ in polar direction, and $0.53°$ in azimuthal direction. Three layer

electromagnetic calorimeter consists of 1632 NaI(Tl) crystals. The energy resolution of the calorimeter for photons is $\sigma_E/E = 4.2\%/\sqrt[4]{E(\text{GeV})}$. The angular resolution is equal to $\sigma_\phi, \sigma_\theta \simeq 1.5°$. The muon system includes scintillation counters and two layers of streamer tubes.

In our analysis, we used the statistics of two experiments, OME9803 and OME0001, collected in 1998–2000. The integrated luminosity in the OME9803 and OME0001 experiments was 3697 and 5881 nb^{-1}, respectively. The integrated luminosity was measured by two independent methods: using events of electron-positron scattering and annihilation into two photons. The systematic uncertainty in the luminosity was estimated as the difference of these two measurements to be approximately 2%.

3   Event selection

For our analysis, we selected events that satisfied the following conditions:

1) two or more charged tracks;

2) four or more reconstructed photons;

3) the distance from the beam axis to the event vertex in the R-ϕ plane is less than 1 cm;

4) the coordinate of the event vertex along the beam axis is less than 10 cm.

The conditions on the vertex coordinates are deter mined by the size of the interaction region, the drift chamber resolution and serve to suppress the beam background events and cosmic muons. The longitudi nal size of the interaction point depends on the beam energy; in the experiment, it changed from 2.0 to 2.5 cm.

The main background process is $e^+e^- \to \pi^+\pi^-\pi^0$ with the overlap with beam background photons or

photons produced by the strong interaction of π-mesons with the detector material and photons emitted from the initial and final states. We also considered the process $e^+e^- \to \eta\gamma$, $\eta \to \pi^+\pi^-\pi^0$, as a background process.

For the events selected under above conditions, we performed kinematic fits in the hypotheses:

- $e^+e^- \to \pi^+\pi^-\pi^0\pi^0$

- $e^+e^- \to \pi^+\pi^-\pi^0$

- $e^+e^- \to \pi^+\pi^-\pi^0\gamma$

In the reconstruction, we used photons satisfying the following conditions:

- minimum photon energy $E_\gamma > 20$ MeV

- photon polar angle $30° < \theta < 150°$

After kinematic fit we used next cuts on likelihood value (Fig. 2):

- $\chi^2_{4\pi} < 40$

- $\chi^2_{3\pi} > 20$

More details about events selection and kinematic fit could be found in [6].

4   Background subtraction

The H-Matrix [7] discriminant was used to separate the events for $\pi^+\pi^-\pi^0\pi^0$ and $\pi^+\pi^-\pi^0$ final states. The following parameters were used to construct the discriminant: the χ^2 of the in the hypothesis $e^+e^- \to \pi^+\pi^-4\gamma$, the invariant masses of two π-mesons composed of four photons taken kinematic fit
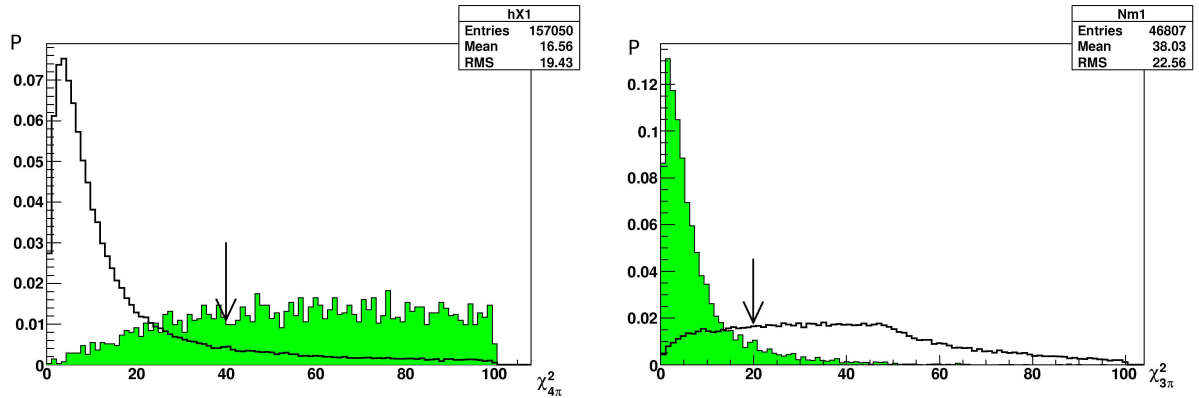

Fig. 2.   Normalized distributions of parameters $\chi^2_{4\pi}$ and $\chi^2_{3\pi}$ for simulated events: the hatched histograms and solid lines are for the processes $\pi^+\pi^-\pi^0$ and $\pi^+\pi^-\pi^0\pi^0$, respectively.
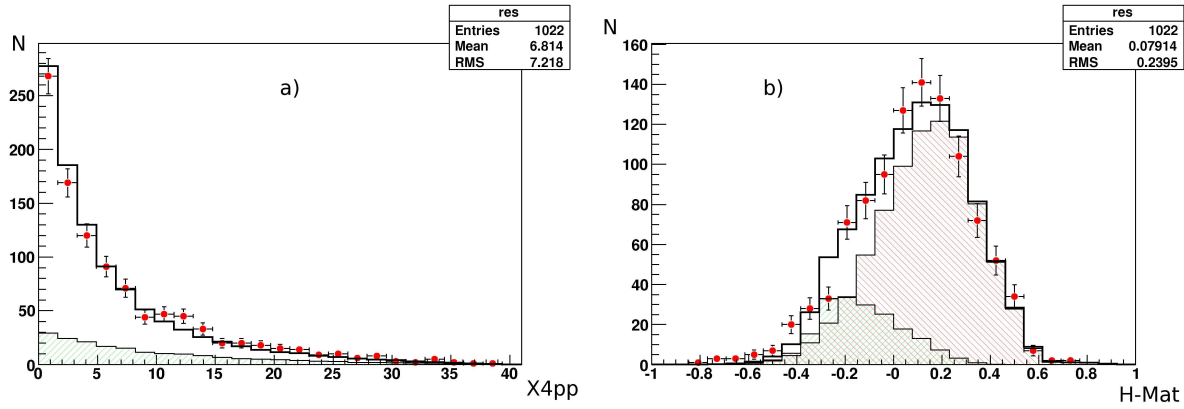
Fig. 3.　Distributions of parameters $\chi^2_{\pi^+\pi^-4\gamma}$ (a) and H-Matrix (b). The points with error bars represent the experimental data; the hatched histograms indicate the simulated $\pi^+\pi^-\pi^0$ background events (\\\) and $\pi^+\pi^-\pi^0\pi^0$ events (///); the lines indicate the sums of all contributions. The events were selected in the energy range 800–1000 MeV.
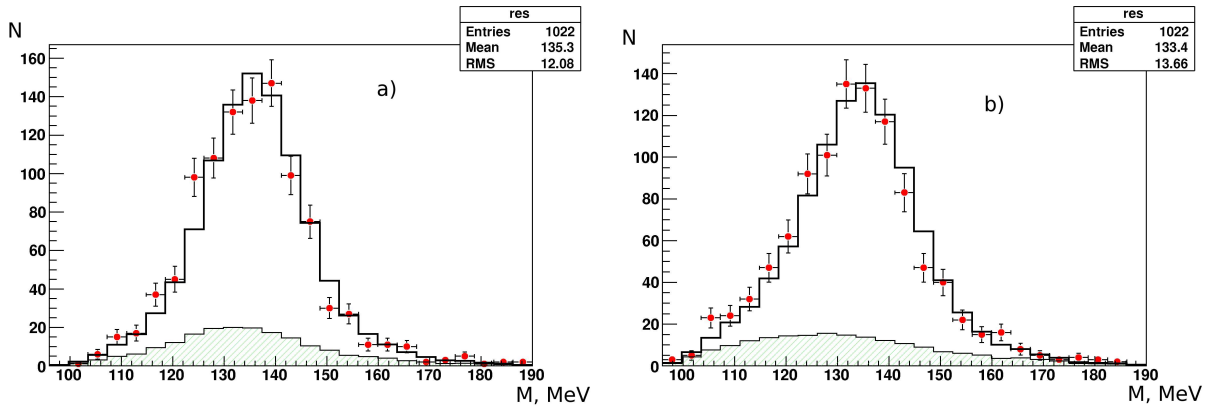

Fig. 4.　Invariant mass distribution of the most energetic (a) and least energetic (b) π^0-mesons after the reconstruction in the model $\pi^+\pi^-4\gamma$. The points with error bars represent the experimental data; the hatched histogram indicate the simulated $\pi^+\pi^-\pi^0$ background events; the lines indicate the sums of all contributions. The events were selected in the energy range 800–1000 MeV.

in the reconstruction $\pi^+\pi^-\pi^0\pi^0$, recoil mass of the photon that was not included in π^0 in the model $\pi^+\pi^-\pi^0\gamma$, the lowest energy and the minimal angle of the photons taken in the reconstruction $\pi^+\pi^-\pi^0\pi^0$ (Fig. 3, Fig. 4).

The discriminant was trained on the simulated events for these processes. All simulated events were divided into two parts: the first part was used to train the algorithm and the second part to test the stability of the response.

The number of events for the process $\pi^+\pi^-\pi^0\pi^0$ at each energy point was determined by fitting the H-Matrix distribution by the sum of the background and signal distributions. We fixed the shape of the background and signal distributions from simulations using the Kernel Estimation method [8]. The fitting was performed by the method of an unbinned maximum likelihood function [9].

To subtract the events of the $\eta\gamma$ background, we

used the recoil mass distribution M_γ (Fig. 5) of the photon that was not included in π^0 in the reconstruction $\pi^+\pi^-\pi^0\gamma$. The events of this background are grouped near the η-meson mass.

Thus, we fitted the two-dimensional distribution of parameters H-Matrix and M_γ by the sum of three distributions: the signal $\pi^+\pi^-\pi^0\pi^0$ and two backgrounds $\pi^+\pi^-\pi^0\gamma$ and $\eta\gamma$. The numbers of signal events and background events were free parameters.

At energies $\sqrt{s} > 880$ MeV, we assumed the presence of two mechanisms of the reaction $e^+e^- \to \pi^+\pi^-\pi^0\pi^0$ with the intermediate states $\omega\pi^0$ and $a_1\pi$. To separate events of the intermediate state $\omega\pi^0$ from others, we used the invariant mass distribution of the system $\pi^+\pi^-\pi^0$ in the reconstruction $\pi^+\pi^-\pi^0\pi^0$ that is closest to the ω-meson mass ($M_{3\pi}$) (Fig. 6).

At energies $\sqrt{s} > 880$ MeV, we fitted the three-dimensional distribution of parameters H-Matrix, M_γ, and $M_{3\pi}$ by the sum of four distributions: two

signals, the mechanisms $\omega\pi^0$ and $a_1\pi$, and two backgrounds, $\pi^+\pi^-\pi^0\gamma$ and $\eta\gamma$.
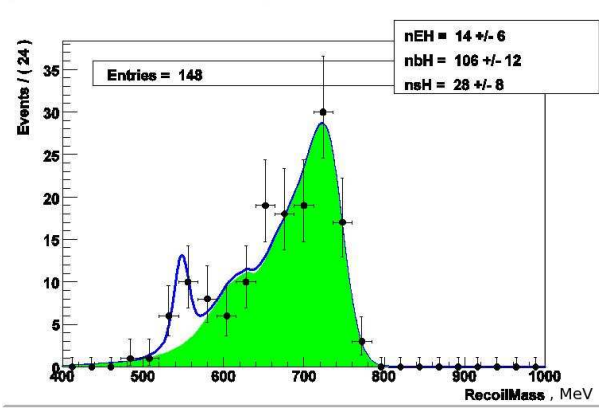

Fig. 5. Distribution of parameter M_γ. The points with error bars represent the experimental data; the gray histogram indicates the sum of the simulated $\pi^+\pi^-\pi^0$ background and $\pi^+\pi^-\pi^0\pi^0$ signal events; the solid curve indicates the fit. The center of mass energy is 784 MeV.
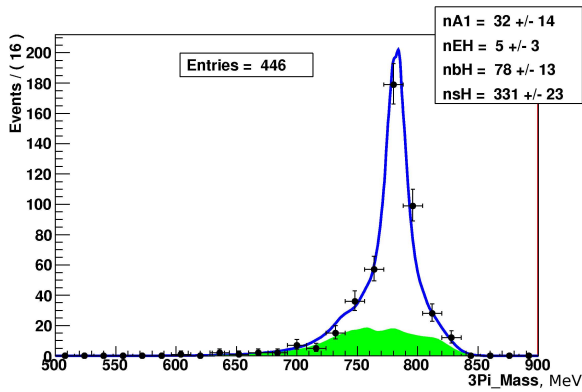

Fig. 6. Distribution of parameter $M_{3\pi}$. The points with error bars represent the experimental data; the gray histogram indicates the sum of the simulated $\pi^+\pi^-\pi^0$ background and $a_1\pi$ signal events; the solid curve indicates the fit. The center of mass energy is 970 MeV.

We determined the detection efficiency by the Monte Carlo method. The mean detection efficiency for the channels $a_1\pi$ and $\omega\pi^0$ is (33.5 ± 0.4) and $(32.5\pm1.4)\%$, respectively.

5   Cross-section approximation

The visible cross section of the process $e^+e^- \rightarrow \pi^+\pi^-\pi^0\pi^0$ at each energy point was determined using the formula:

$$\sigma_{\mathrm{vis}}(E) = \frac{N_{4\pi}(E)}{IL(E)\cdot\varepsilon(E)}, \qquad (1)$$

where $N_{4\pi}$ is the number of events for the process under study, $IL(E)$ is the integrated luminosity at a given point, and $\varepsilon(E)$ is the detection efficiency.

The visible cross section was approximated by a theoretically expected one:

$$\sigma_{\mathrm{th}}(E) = \int\limits_0^{X_{\max}} \mathrm{d}z\cdot\sigma_{\mathrm{born}}(E(1-z))\cdot F(z,E). \qquad (2)$$

Here, $\sigma_{\mathrm{born}}(E)$ is the Born cross section, the function F describes the probability of losing the fraction of energy z through the emission of photons from the initial state. The radiative correction was calculated using the formula:

$$\delta_{\mathrm{rad}} = \frac{\sigma_{\mathrm{th}}(E)}{\sigma_{\mathrm{born}}(E)} - 1. \qquad (3)$$

We parameterized the Born cross section at $\sqrt{s} > 880$ MeV for the mechanism $\omega\pi^0$ based on the model of vector dominance by taking into account the ρ-meson and two its excitations:

$$\sigma_{\mathrm{born}}(E) = \frac{4\pi\alpha^2}{E^3}\frac{g_{\rho\omega\pi}}{f_\rho}\cdot\left| A_\rho\frac{m_\rho^2}{D_\rho(E)} + A_{\rho'}\cdot\frac{m_{\rho'}^2}{D_{\rho'}(E)} + \right.$$
$$\left. A_{\rho''}\cdot\frac{m_{\rho''}^2}{D_{\rho''}(E)} \right|^2\cdot P_\rho(E), \qquad (4)$$

where $D_\rho(E) = m_\rho^2 - E^2 - iE\Gamma_\rho(E)$ α is the fine-structure constant, $g_{\rho\omega\pi}$ and f_ρ are coupling constants, and m_ρ are the masses of corresponding mesons. The phase space $P_\rho(E)$ was taken from [10].
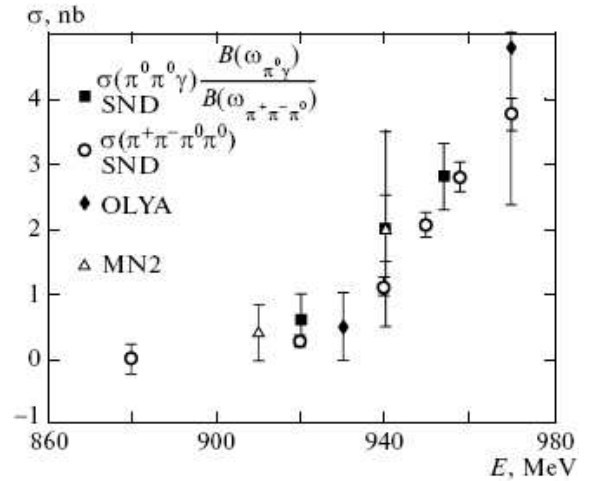

Fig. 7. Cross section of the reaction $e^+e^- \rightarrow \pi^+\pi^-\pi^0\pi^0$ in comperison to previous experiments.

In the approximation, $A_\rho, A_{\rho'}, A_{\rho''}$ – the amplitudes at the energy peak of the corresponding ρ-meson were free parameters. The obtained Born cross

sections are compared with previous experiments in (Fig. 7). We see that the cross section obtained here agrees with previous measurements but has a better accuracy.

At $E < 880$ MeV, the cross section for the process $e^+e^- \to \pi^+\pi^-\pi^0\pi^0$ has been measured for the first time (Fig. 8). Several models were tested at these energies. We have chousen the model where the cross section was approximated by the direct sum of ρ and ω resonances for decay probability measurment:

$$\sigma_{\text{born}}(E) = \frac{4\pi\alpha^2}{E^3}\frac{P_\rho(E)}{|D_\rho(E)|^2} + \frac{4\pi\alpha^2}{E^3}\frac{P_\omega(E)}{|D_\omega(E)|^2}, \quad (5)$$

where $P_\rho(E)$ and $P_\omega(E)$ are the phase space factors for the ρ and ω resonances, respectively; $D_\rho(E)$ and $D_\omega(E)$ are the inverse propagators.

The phase space factor for the ω-meson was calculated in the model $e^+e^- \to \pi^+\pi^-\pi^0$, which corresponds to the main background process. The cross sections at the peak of the resonances were free parameters; the following values were obtained for them: $\sigma_\rho = (1.84 \pm 0.85) \times 10^{-2}$ nb and $\sigma_\omega = (1.83 \pm 0.34) \times 10^{-1}$ nb at $\chi^2 = 28.1/38$. Using the formula for the cross section at the resonance peak,

$$\sigma_0 = \frac{12\pi B_{\text{ee}} B_{4\pi}}{M^2}, \quad (6)$$

where M is the mass of the corresponding resonance and B_{ee} is the e^+e^- decay probability, we obtain

$$B_\rho = (1.60 \pm 0.74) \times 10^{-5} B_\omega = (1.06 \pm 0.20) \times 10^{-4}$$
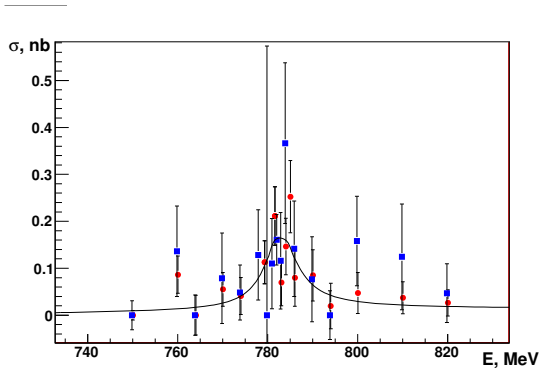

Fig. 8.　Cross section for the reaction $e^+e^- \to \pi^+\pi^-\pi^0\pi^0$. The solid curve indicates the fit.

We also try model with existence of interference between the ρ and ω resonances with a free phase. The third model suggested the existence of interference between the ρ and ω resonances with a free phase, as in the second model, but with the contribution of the direct ω-meson decay. The cros ssections at the peak of the resonances: σ_ρ, $\sigma_{\omega\text{int}}$, $\sigma_{\omega\text{free}}$ and the interference phase, four parameters at all, were free parameters in third model.

The following values of the parameters were obtained: $\sigma_\rho = (1.5 \pm 0.79) \times 10^{-2}$ nb, $\sigma_{\omega\text{int}} = (1.05^{+0.39}_{-1.05}) \times 10^{-1}$ nb, $\phi_{\rho\omega} = -7.12° \pm 30.6°$ and $\sigma_{\omega\text{free}} < 0.23$ nb at $\chi^2 = 27.7/36$. In this case, the likelihood function has a continuous set of minima, since the parameters $\sigma_{\omega\text{int}}$ and $\sigma_{\omega\text{free}}$ are strongly correlated. The upper limit for the decay $\omega \to \pi^+\pi^-\pi^0\pi^0$, corresponding to $\sigma_{\omega\text{free}} < 0.23$ nb is $B_\omega < 2 \times 10^{-4}$ at 90% confidence level.

The radiative correction to the cross section was calculated using the first model; the cross section for the ω-resonance was assumed to be the background one and was not included in our calculation of the radiative correction. Tables with cross section could be found at Ref. [6].

6　Systematic uncertainties

To estimate the systematic errors related to the selection criteria, we rejected one selection criterion at a time and performed the signal/background separation procedure again. The change in the cross section when rejecting one of the selection criteria is shown in Fig. 9. The systematic uncertainty measured in this way is 1.9%. The systematic uncertainties related to the luminosity measurement, 2%, and the radiative correction calculation, 1%, should also be added to it.
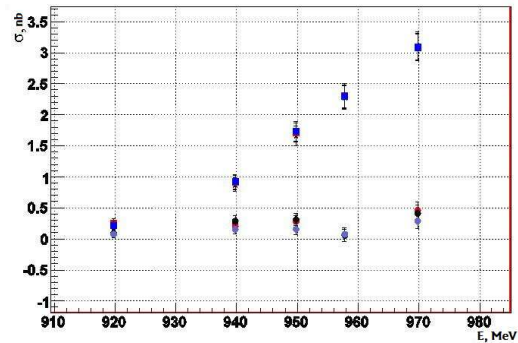

Fig. 9.　Cross section for the reaction $e^+e^- \to \pi^+\pi^-\pi^0\pi^0$. Squares – all selection criteria were imposedions, sircles – selection criterion $\chi^2_{4\pi} < 40$ was rejected, stars – $\chi^2_{3\pi} > 20$ was rejected.

Particular attention was paid to the region of the ω-meson peak (778–788 MeV). To found the systematic uncertainty, we proceeded here just as in the energy range 920–980 MeV, i.e., we rejected each of the selection criteria one by one and performed the background subtraction procedure again. A systematic bias in the cross section was found; the cross section increased by 0.119 ± 0.114 nb.

The significant systematic bias in the ω-meson peak can be explained by the presence of an effect disregarded in our simulations or by an unknown mechanism of the decay $\omega \to \pi^+\pi^-\pi^0\pi^0$.

Using the available statistics, we cannot study the angular distributions and the distributions of invariant masses in the ω-meson region and establish experimentally, which effect we observe. The situation is also complicated by the fact, that there are no theoretical predictions for the decay $\omega \to \pi^+\pi^-\pi^0\pi^0$. It is possible that the situation will be clarified in future experiments on VEPP–2000, where several thousand such events instead of several tens of currently available ones are expected. Based on our measurements, we cannot assert that the interfering decay $\omega \to \pi^+\pi^-\pi^0\pi^0$ exists. The entire contribution from the ω-meson is assumed to be related to the background. At our level of accuracy, we use the first model to calculate the radiative correction. In this case, the difference of the radiative corrections for the first and second models can reach 11%.

7   Conclusion

We measured the cross section for the process

$e^+e^- \to \pi^+\pi^-\pi^0\pi^0$ in the experiment with SND detector at the VEPP–2M collider. In the energy range $920 < \sqrt{s} < 980$ MeV the measurement has the best accuracy to date; the systematic uncertainty is considerably smaller than the statistical one. At energies $\sqrt{s} < 920$ MeV, this cross section has been measured for the first time.

The $\rho \to \pi^+\pi^-\pi^0\pi^0$ decay probability was found to be $B_\rho = (1.60\pm0.74\pm0.18)\times10^{-5}$. The upper limit for the decay $\omega \to \pi^+\pi^-\pi^0\pi^0$ was improved by two orders of magnitude compared to previous measurements and is $B_\omega < 2\times10^{-4}$ at 90% confidence level. These results should be compared with the Particle Data Group data of 2008, which give the following upper limits: $B_\rho < 4\times10^{-5}$ and $B_\omega < 2\times10^{-2}$. It can be seen that we have managed to suppress the 3π background by two orders of magnitude better than in previous works and to measure the probability of the decay $\rho \to \pi^+\pi^-\pi^0\pi^0$.

References

1 Kurdadze L M et al. Pis'ma Zh. Eksp. Teor. Fiz., 1986, **43**(11): 497 [JETP Lett., 1986, **43**(11): 643]
2 Akhmetshin R R et al. Phys. Lett. B, 2000, **475**: 190
3 Yao W M et al (Particle Data Group). J. Phys. G, Nucl. Part. Phys., 2006, **33**: 1
4 Achasov M N et al. Nucl. Instrum. Methods Phys. Res. A, 2000, **449**: 125
5 Skrinsky A N. In Proceedings of the Workshop on Physics and Detectors for DAPHNE, Frascati, Italy. 1995. 3
6 Achasov M N et al. JETP, 2009, **109**(3): 379–392
7 Hocker A et al. arXiv:physics/0703039, http://tmva.sf.net
8 Cranmer K S. Comput. Phys. Commun., 2001, **136**: 198; arXiv:hepex/0011057v1
9 Verkerke W, Kirkby D. arXiv:physics/0306116
10 Aul'chenko V M et al. Zh. Eksp. Teor. Fiz., 2000, **117**(6): 1067 [JETP, 2000, **90**(6): 927]; Druzhinin V P. Doctoral Dissertation in Physics (Budker Institute of Nuclear Physics, Novosibirsk. 2000